A dynamic surface model for segmentation of cardiac MRI images and its usage in cardiac wall motion tracking

[1]F. Jamali Dinan, [1]P. Mosayebi, [1]H. Abrishami Moghaddam, [2]M. Giti

[1] EE Dept. K.N. Toosi Univ . of Technology, P.O.Box 16315-1355, Tehran, Iran
Email: fjdinan2001@yahoo.com, pmosayebi@yahoo.com, moghadam@saba.kntu.ac.ir

[2] Tehran Univ. of Medical Science, Medical Imaging Center/Imam Hospital, Tehran, Iran
Email: m_giti@yahoo.com

Abstract. *This paper presents the application of a new active contour algorithm for object detection in 3D space. The introduced model is based on techniques of curve evolution for segmentation and level sets. We minimize an energy which can be considered as a particular case of the minimal partition problem. In the level set formulation, the problem becomes a "mean-curvature flow"-like evolving the active contour, which will stop on the desired boundary. However, the stopping term does not depend on the gradient of the image, as in the classical active contour models, but is instead related to a particular segmentation of the image. The method can be put into a 3D level-set framework using a Lipschitz function ϕ for automatic topology changes. The novel developed 3D algorithm was used for 3D segmentation of endocardial wall in the left ventricle. The experimental results demonstrated the efficiency of the proposed scheme. The segmented cardiac image was then used by our previously developed 3D tracking algorithm to track the endocardial wall motion which resulted in a fully automatic 3D point-wise tracking software for analyzing 3D cardiac MRI images.*

Keywords*: deformable surface, level set, active mesh, cardiac image*

1. Introduction

Segmentation of the left ventricle is of great clinical interest, since it is the first step in analyzing cardiac images. Primary works on automatic segmentation of cardiac images were based on simple techniques such as thresholding or region growing [1]. However these methods could not represent subvoxel resolution. Some more elaborated approaches were probabilistic or statistical [2,3]. A disadvantage of probabilistic models is that they require a learning database to adapt themselves with the pathology. Therefore, this imagebase should be relatively large. Furthermore, the database is image modality dependent and so it is cumbersome to apply the algorithm to new types of image data. A recent segmentation model which is useful in cardiac images is level set model [4]. The level set model is problematic in including a priori information and also is computationally intensive for 3D+T cardiac data sets. Another segmentation algorithm is 3D active appearance model [5]. This model has problems of coping with shape variability outside the learning set, and it is computationally expensive to have a learning set that includes all phases of the cardiac cycle. Deformable models or active contours [6,7] and snake models rely on the edge-function, depending on the image gradient to stop the curve evolution. Chan and Vese proposed a different active contour

model which was not based on the gradient of the image for the stopping process [8]. Their model could detect contours either with or without gradient, for instance objects with very smooth boundaries or even with discontinuous boundaries. However, their model was presented in the two dimensional space [8].

We have previously developed a fully 3D active mesh model based on a finite-element deformable volume to achieve efficient representation of global and local deformations [9]. However, an accurate and efficient 3D segmentation algorithm was needed for automation of the tracking algorithm. In this paper, we have introduced a fully 3D surface detection algorithm and used it for detection of cardiac wall in the left ventricle for the first phase of cardiac cycle in MRI images. The extracted surface was then used by the tracking algorithm for point-wise tracking of the cardiac wall motion which resulted in a fully automatic 3D point-wise tracking software for analyzing 3D cardiac MRI images. This paper is organized as follows. In section 2, we formulate the 3D object detection model. In section 3, we use the algorithm for MR cardiac images and then use the results for tracking cardiac motion. Finally in section 4, conclusions are drawn.

2. Object detection

Let I be a 3D image and B is an object located in I .We propose a 3D model for active contours to detect object B , based on techniques of curve evolution. For this purpose, we consider the initial surface as a sphere which could be anywhere in I . The initial sphere starts deforming until it stops on the desired boundary.

2.1 Algorithm development

Let Ω be a bounded open subset of R^3, with $\partial\Omega$ its boundary and u_0 be a given 3D image, $u_0 : \Omega \to R$ .Let us define the evolving Surface S in Ω , as the boundary of an open subset of ω (i.e. $\omega \subset \Omega$ and $S = \partial\omega$). In what follows, inside S denotes the region ω , and outside denotes the region $\Omega - \omega$ .Consider a simple case where the 3D image u_0 is formed by two regions of piecewise constant intensity. Denote the intensity values by u_0^o and u_0^i .Furthermore, assume that the object to be detected has a region whose boundary is S_0 and its intensity is u_0^i . Then, consider the following "fitting" term:

$$F_1(S) + F_2(S) = \int_{inside\ (S)} |u_0(x,y,z) - c_1|^2 \, dxdydz + \int_{outside\ (S)} |u_0(x,y,z) - c_2|^2 \, dxdydz \tag{1}$$

The constants c_1 and c_2 are the averages of u_0 inside and outside S , respectively. If the surface S is outside the object, $F_1(S) \approx 0$ and $F_2(S) > 0$. In case that S is inside the object then, $F_1(S) > 0$ and $F_2(S) \approx 0$. If S is both inside and outside of the object then, $F_1(S) > 0$ and $F_2(S) > 0$. Finally, the fitting energy is minimized if $S = S_0$, i.e. if the surface S is the boundary of the object.

$$\inf_c \{F_1(S) + F_2(S)\} \approx 0 \approx F_1(S_0) + F_2(S_0) \tag{2}$$

In our 3D active contour model, we will minimize the above fitting term and will add some regularizing terms to (1) to introduce the energy functional $F(c_1, c_2, S)$, defined by:

$$\begin{aligned} F(c_1,c_2,S) &= \mu \cdot Area(S) + \nu \cdot Volume(inside(S)) \\ &+ \lambda_1 \int_{inside(S)} |u_0(x,y,z) - c_1|^2 dxdydz \\ &+ \lambda_2 \int_{outside(S)} |u_0(x,y,z) - c_2|^2 dxdydz \end{aligned} \tag{3}$$

where $\lambda_1 > 0$, $\lambda_2 > 0$, $\nu \geq 0$ and $\mu \geq 0$ are fixed parameters.

Now we want to find the values of c_1, c_2 and S so that $F(c_1,c_2,S)$ is minimized. This problem can be formulated using level sets as follows. The evolving surface S can be represented by the zero level set of the signed distance function (Lipschitz function) $\varphi : \Omega \to R^3$ as in (4)

$$\begin{cases} \varphi(x,y,z,t=0) = \pm d \\ S = \partial w = \{(x,y,z) \in \Omega, \varphi(x,y,z,) = 0\} \\ \text{inside}(S) = w = \{(x,y,z) \in \Omega, \varphi(x,y,z,) > 0\} \\ \text{outside}(S) = w = \{(x,y,z) \in \Omega, \varphi(x,y,z,) < 0\} \end{cases} \tag{4}$$

In (4), d is the distance of (x,y,z) with boundary surface $\partial\omega$ in $t=0$. Therefore, we replace the unknown variable S by φ. Now consider the Heaviside function H, and the Dirac measure δ:

$$H(z) = \begin{cases} 1, & z \geq 0 \\ 0, & z < 0 \end{cases}, \qquad \delta(z) = \frac{d}{dz} H(z) \tag{5}$$

We can rewrite the lateral surface $\varphi = 0$ and the inside regions $\varphi = 0$ with these functions. As H is positive inside the boundary surface and is zero in other regions, the volume of the inside regions will be the integral of $H(\varphi)$. The gradient of H defines the boundary surface. So summation of it on the assumed region defines the outside boundary surface, mathematically:

$$\begin{aligned} Volume\ \{\varphi > 0\} &= \int_\Omega H(\varphi(x,y,z)) dxdydz \\ Area\ \{\varphi = 0\} &= \int_\Omega \nabla H(\varphi(x,y,z)) dxdydz \\ &= \int_\Omega \delta_0(\varphi(x,y,z)) |\nabla \varphi(x,y,z)| dxdydz \ , \end{aligned} \tag{6}$$

Similarly, we can rewrite the previous energy equations so that they are defined over the entire domain Ω rather than separated into inside(S): $\varphi \geq 0$ and outside (S) : $\varphi < 0$ Then, the energy $F(c_1,c_2,S)$ can be written as:

$$\begin{aligned} & F(c_1,c_2,S) \\ &= \mu \int_\Omega \delta(\varphi(x,y,z)) |\nabla \varphi(x,y,z)| dxdydz \\ &+ \nu \int_\Omega H(\varphi(x,y,z)) dxdydz \\ &+ \lambda_1 \int_\Omega |u_0(x,y,z) - c_1|^2 H(\varphi(x,y,z)) dxdydz \\ &+ \lambda_2 \int_\Omega |u_0(x,y,z) - c_2|^2 (1 - H(\varphi(x,y,z))) dxdydz \end{aligned} \tag{7}$$

The constants c_1 and c_2 are the average of u_0 in $\varphi \geq 0$ and $\varphi < 0$, respectively. So they are easily computed as:

$$c_1(\varphi) = \frac{\int_\Omega u_0(x,y,z) H(\varphi(x,y,z)) dxdydz}{\int_\Omega H(\varphi(x,y,z)) dxdydz} \tag{8}$$

$$c_2(\varphi) = \frac{\int_\Omega u_0(x,y,z)(1 - H(\varphi(x,y,z))) dxdydz}{\int_\Omega (1 - H(\varphi(x,y,z))) dxdydz} \tag{9}$$

Keeping c_1 and c_2 fixed, and minimizing F with respect to φ, we can deduce the Euler–Lagrange partial differential equation from (7). We parameterize the descent direction by $t > 0$, so the equation $\varphi(x,y,z,t)$ is:

$$\frac{\partial \varphi}{\partial t} = \delta(\varphi) \cdot \left[\mu \cdot div\left(\frac{\nabla \varphi}{|\nabla \varphi|} \right) - \nu - \lambda_1 (u_0 - c_1)^2 + \lambda_2 (u_0 - c_2)^2 \right] = 0, \tag{10}$$

For solving the above equation, we first need to regularize $H(z), \delta(z)$. Chan and Vese [8] propose:

$$H_\varepsilon(z) = \frac{1}{2} + \frac{1}{\pi} \arctan\left(\frac{z}{\varepsilon} \right), \quad \delta_\varepsilon(z) = \frac{1}{\pi} \cdot \frac{\varepsilon}{\varepsilon^2 + z^2} \tag{11}$$

Chan and Vese [8] give the following discretization and linearization of (10):

$$\begin{aligned}
&\frac{\varphi_{i,j,k}^{n+1} - \varphi_{i,j,k}^{n}}{\Delta t} = \delta_\varepsilon\left(\varphi_{i,j,k}^{n}\right) \left[\frac{\mu}{h^2} \Delta \underline{x} \right. \\
&\cdot \left(\frac{\overset{x}{\Delta} + \varphi_{i,j,k}^{n+1}}{\sqrt{\left(\overset{x}{\Delta} + \varphi_{i,j,k}^{n}\right)^2 \Big/ \left(h^2\right) + \left(\varphi_{i,j+1,k}^{n} - \varphi_{i,j-1,k}^{n}\right) \Big/ (2h)^2 + \left(\varphi_{i,j,k+1}^{n} - \varphi_{i,j,k-1}^{n}\right) \Big/ (2h)^2}} \right) \\
&+ \frac{\mu}{h^2} \Delta \underline{y} \\
&\cdot \left(\frac{\overset{y}{\Delta} + \varphi_{i,j,k}^{n+1}}{\sqrt{\left(\varphi_{i+1,j,k}^{n} - \varphi_{i-1,j,k}^{n}\right) \Big/ (2h)^2 + \left(\overset{y}{\Delta} + \varphi_{i,j,k}^{n}\right)^2 \Big/ \left(h^2\right) + \left(\varphi_{i,j,k+1}^{n} - \varphi_{i,j,k-1}^{n}\right) \Big/ (2h)^2}} \right) \\
&+ \frac{\mu}{h^2} \Delta \underline{z} \\
&\cdot \left(\frac{\overset{z}{\Delta} + \varphi_{i,j,k}^{n+1}}{\sqrt{\left(\varphi_{i+1,j,k}^{n} - \varphi_{i-1,j,k}^{n}\right) \Big/ (2h)^2 + \left(\varphi_{i,j+1,k}^{n} - \varphi_{i,j-1,k}^{n}\right) \Big/ (2h)^2 + \left(\overset{z}{\Delta} + \varphi_{i,j,k}^{n}\right)^2 \Big/ \left(h^2\right)}} \right) \\
&\left. - \nu - \lambda_1 \left(u_{0,i,j,k} - c_1\left(\phi^n\right)\right)^2 + \lambda_2 \left(u_{0,i,j,k} - c_2\left(\phi^n\right)\right)^2 \right]
\end{aligned} \tag{12}$$

where the forward differences of $\varphi_{h,j,k}^{n}$ are calculated according to (13).

$$\begin{aligned}
&\overset{x}{\Delta-}\varphi_{i,j,k} = \varphi_{i,j,k} - \varphi_{i-1,j,k}, \overset{x}{\Delta+}\varphi_{i,j,k} = \varphi_{i+1,j,k} + \varphi_{i,j,k} \\
&\overset{y}{\Delta-}\varphi_{i,j,k} = \varphi_{i,j,k} - \varphi_{i,j-1,k}, \overset{y}{\Delta+}\varphi_{i,j,k} = \varphi_{i,j+1,k} + \varphi_{i,j,k} \\
&\overset{z}{\Delta-}\varphi_{i,j,k} = \varphi_{i,j,k} - \varphi_{i,j,k-1}, \overset{z}{\Delta+}\varphi_{i,j,k} = \varphi_{i,j,k+1} + \varphi_{i,j,k}
\end{aligned} \tag{13}$$

The segmentation algorithm is then:

1) In 3D image sequences the "Volume of Interest" is defined.

2) We assume the initial surface φ^0 in φ_0 and also $n=0$.

3)for fixed number of iterations do

- $c_1(\varphi^n)$and $c_2(\varphi^n)$ are obtained from (8) and (9).
- φ^{n+1} is computed from (12).

end

4)This algorithm adopted for segmentation of the endocardium ,hence Segmentation of the cardiac external wall is done manually by the operator.

5) We filter the segmented image to eliminate noisy regions of the surface, for example the resulted regions which correspond to papillary muscles

6) We use linear interpolation to convert the voxels to cube elements.

7) The segmentation result of the first frame is used for the active mesh software.

3. Result

We evaluated the algorithm on cardiac images. In Fig. 1, we have shown the segmentation of the first phase of 4D gradient-echo images. In Fig. 2 epicardial and endocardial contours of these images are shown and in Fig. 3 the surface of cardiac wall resulted by the segmentation algorithm in the first phase of gradient-echo images is shown.

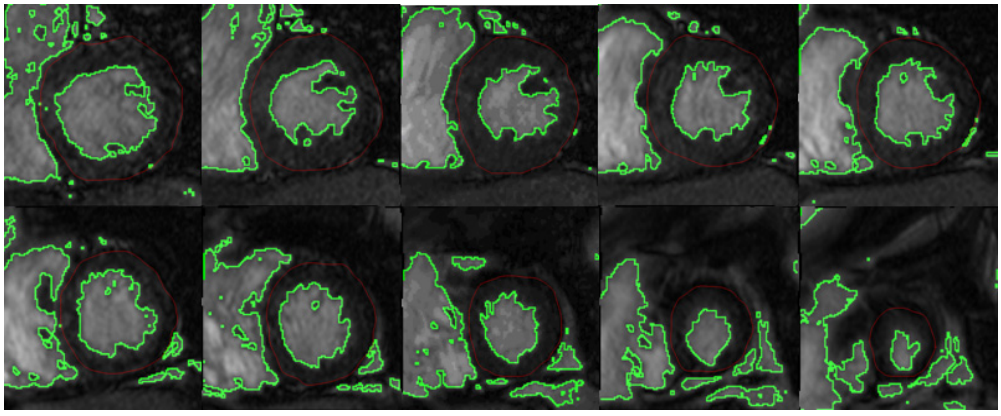

Fig. 1. Segmentation of gradient-echo images

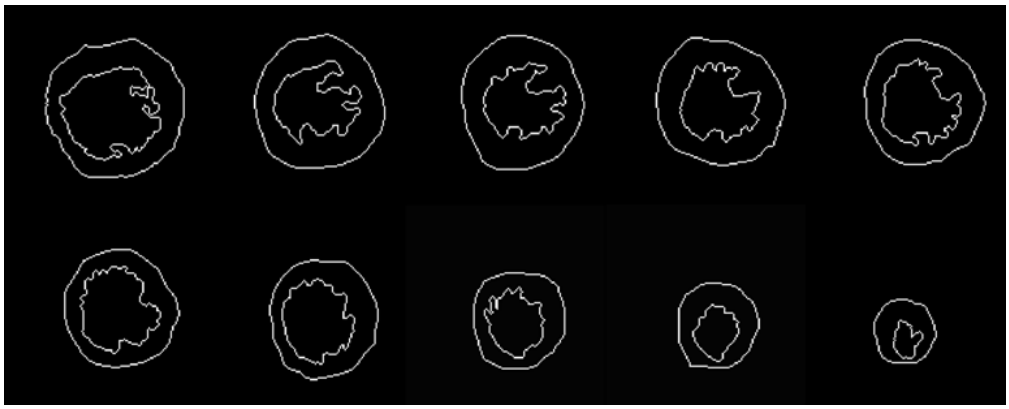

Fig. 2. Epicardial and endocardial contours

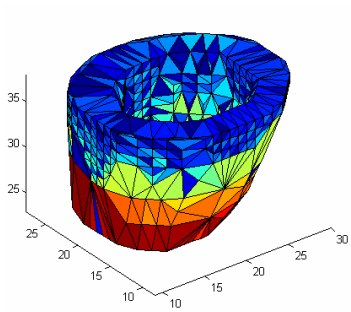

Fig. 3. The surface of cardiac wall

The obtained surface of the first phase of cardiac cycle is then used by active mesh algorithm to track the cardiac wall motion [9]. In Fig. 4, the result of tracking of the left ventricle wall by active mesh algorithm in Gradient-echo image is shown. The results show that the algorithm can track the cardiac motion in all 3 dimensions with significant resolution.

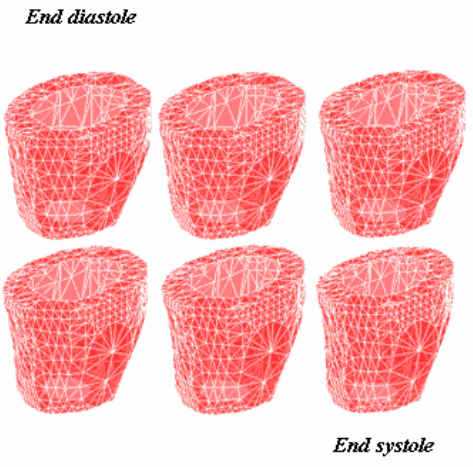

Fig. 4. Tracking the wall of left ventricle

For quantitative evaluation of the algorithm performance in tracking the internal cardiac walls, the tracked surfaces obtained by the algorithm and the surfaces extracted by segmentation software were compared. The comparison was done by finding the similarity index between two surfaces [9]. The obtained errors are shown in Table 1.

Table 1. The tracking algorithm error

Frame	2	3	4	5	6	7
Error (%)	4.3	4.71	5.15	4.71	4.27	4.1

4. Conclusion

In this paper, we developed a 3D segmentation algorithm based on a levelset approach. Our model is not based on an edge-function to stop the evolving curve on the desired boundary. Also, we do not need to smooth the initial image, even if it is very noisy and in this way, the locations of boundaries are very well detected and preserved. For automatic segmentation of cardiac walls, we have enhanced our previously developed tracking software. Further enhancements of tracking software could be conducted in order to model cardiac muscle anisotropy and nonlinearity. In addition, the present correlation-based search method may be improved for the estimation of tangential motion in the consecutive frames. Shape-based tracking algorithms seem to be better choices for perpendicular and tangential motion estimation. Finally, a regularization term can be added to these equations for reducing the computational cost as well as obtaining a more robust estimation of deformation fields.

Acknowledgements

The authors would like to thank Mr. Saeed Kermani from Amirkabir University for providing 3-D cardiac MRI image data for this study.

References

[1] Maes L., Bijnens B., Suetens P., Werf F. V. D. : Automated contour detection of the left ventricle in short axis view in 2d echocardiograms, Machine Vision and Applications 6 (1993) 1–9.

[2] Dias J. M. B., Leitao J. M. N.:Wall position and thickness estimation from sequences of echocardiographic images, IEEE Transactions on Medical Imaging 15 (1) (1996) 25–38.

[3] Lorenzo-Valdes M., Sanchez-Ortiz G. I., Elkington A. G., Mohiaddin R. H., Rueckert D.: Segmentation of 4D cardiac MR images using a probabilistic atlas and the EM algorithm, Med Image Anal. 8 (3) (2004) 255–65.

[4] Paragios N. : A level set approach for shape-driven segmentation and tracking of the left ventricle, IEEE Trans. Med. Imag. 22 (6) (2003) 773–776.

[5] Mitchell S. C., Bosch J. G., Lelieveldt B. P., van der Geest R. J., Reiber J. H., Sonka M.: 3-D active appearance models: segmentation of cardiac MR and ultrasound images, IEEE Trans. Med. Imag. 21 (9) (2002) 1167–78.

[6] McInerney T., Terzopoulus D.: A dynamic finite element surface model for segmentation and tracking in multidimensional medical images with application to cardiac 4d image analysis, Computerized Medical Imaging and Graphics 19 (1) (1995) 69–83.

[7] Kaus M. R., Berg Jv J. , Weese J., Niessen W., Pekar V.: Automated segmentation of the left ventricle in cardiac mri, Med Image Anal 8 (3) (2004) 245–54.

[8] Chan T. and Vese L.:Active contours without edges. IEEE Trans. Image Proc., 10(2):266-277, 2001.

[9] Mosayebi P., Abrishami Moghaddam H., and Giti: A Fully 3D Active Mesh Model for MotionTracking in Cardiac MRI. MICCAI international workshop, Denmark, Oct. 2006.